Plasmon excitation in metallic spheres

N. Barberán and J. Bausells
Departamento de Optica, Facultad de Fisica, Universidad de Barcelona, 08028 Barcelona, Spain
(Received 6 February 1984; revised manuscript received 18 July 1984)

A detailed study is presented of the influence of several parameters on the energy-loss probability of fast electrons (~ 100 keV) incident on small metallic spherical particles. We consider the collective modes of the sphere, including bulk-type modes which do not appear to have been considered previously in the literature. A Gaussian distribution is used to describe the electron in the plane transverse to the trajectory. We discuss the effects of the variation of several parameters—incident beam size, probe velocity, radius of the sphere, impact parameter, and the excited mode—and conclude that the absorption spectra depend critically on the geometry of the probe as the experimental data of Batson and Treacy suggest.

I. INTRODUCTION

The problem of inelastic scattering of fast electrons passing through or nearby small spherical particles has been studied by a number of authors. The incident electron is represented either as a plane wave[1] or as a point classical particle with an eventual averaging over impact parameter.[2] The recent development of high-resolution scanning-transmission electron microscopy (STEM) has renewed the interest in this problem. STEM has made available a technique of electron energy spectroscopy in highly localized regions of inhomogeneous specimens.[3] Schmeits[4] has calculated the excitation probability of the $l=1$ and 2 surface modes by a 50-keV classical electron scattered from a free-electron sphere with a well-defined impact parameter, the bulk plasmon excitation probability being obtained by a closure relation.

In this work we use a free-electron model to describe the response of the medium with explicit inclusion of nonlocal dispersive effects. In Sec. II we analyze in detail the bulk and surface excited modes. In Sec. III we compare the predictions of a theory treating the incident particle classically with those obtained by a more realistic quantum approach where the electron makes a transition from an incident state, highly localized in two dimensions, to a plane-wave final state describing a situation in which the scattered electron is collected in a spectrometer with an entrance aperture subtending a half angle of $\theta \simeq 5$ mrad at the specimen. A discussion of our results is presented in Sec. IV.

II. NORMAL MODES

In the hydrodynamical model a set of linearized equations[5] is written for the fluctuations in the electron density n, electrostatic and velocity potentials ϕ and ψ.

$$\frac{\partial}{\partial t}\nabla\psi = -\nabla\phi + \frac{\beta^2}{n_0}\nabla n \ , \tag{1}$$

$$\nabla^2\phi = 4\pi n \ , \tag{2}$$

$$\nabla^2\psi = \frac{1}{n_0}\frac{\partial}{\partial t} n \ . \tag{3}$$

Here n_0 is the mean electron density; the value of $\beta(\beta^2 = 3v_F^2/5)$ is taken to reproduce the random-phase-approximation bulk plasmon dispersion relation, v_F being the Fermi velocity of the electron gas. We ignore retardation and damping effects and use atomic units throughout ($e=\hbar=m=1$).

The normal mode solutions of frequency ω_α (α denotes angular and radial components) satisfy the equation

$$\nabla^2 n + k^2 n = 0 \ , \tag{4}$$

where

$$k^2 = (\omega_\alpha^2 - \omega_p^2)/\beta^2 \tag{5}$$

with ω_p the bulk plasma frequency.

The solutions of Eq. (4) can be written as

$$n(\mathbf{r},t) = \sum_\alpha A_\alpha j_l(kr) Y_{lm}(\theta,\varphi) e^{-i\omega_\alpha t} + \text{H.c.} \ , \tag{6}$$

where (r,θ,φ) are the polar coordinates, j_l is the spherical Bessel function, and Y_{lm} the spherical harmonic.

Using Eq. (6) for n, together with the continuity of ϕ and its radial derivative at the surface ($r=R$) of the sphere, we obtain for the electrostatic potential ϕ

$$\phi(\mathbf{r},t) = \sum_\alpha B_\alpha \left[j_l(kr) - \frac{kR}{2l+1} j_{l-1}(kR) \left[\frac{r}{R} \right]^l \right] \times e^{-i\omega_\alpha t} Y_{lm}(\theta,\varphi) + \text{H.c.}, \quad r \le R \tag{7}$$

and

$$\phi(\mathbf{r},t) = \sum_\alpha B_\alpha \frac{kR}{2l+1} \left[\frac{R}{r} \right]^{l+1} j_{l+1}(kR) \times e^{-i\omega_\alpha t} Y_{lm}(\theta,\varphi) + \text{H.c.}, \quad r \ge R \tag{8}$$

where the constants A_α and B_α are related by $4\pi A_\alpha = -k^2 B_\alpha$.

The mode frequencies ω_α are fixed by the additional boundary condition that the radial velocity $\partial\psi/\partial r$ should vanish at $r=R$. This follows from the requirement that

 ©1985 The American Physical Society

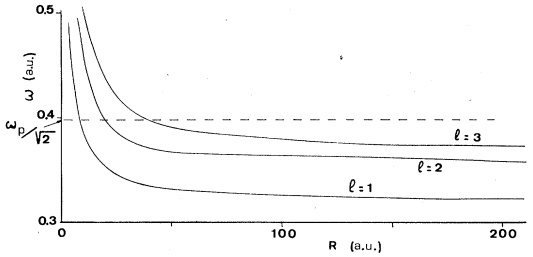

FIG. 1. Surface plasmon frequency dependence upon the sphere radius R, for several values of l.

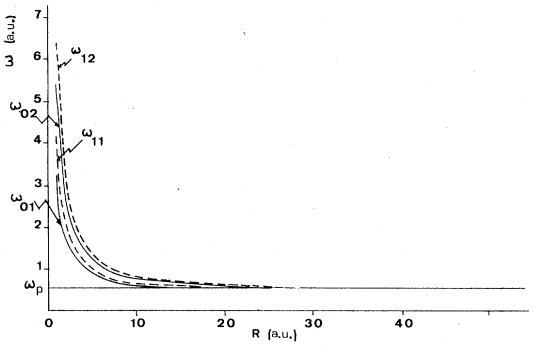

FIG. 2. Bulk plasmon frequency as a function of the sphere radius R for several values of l and ν.

charge and current densities should be finite everywhere.[6] After some algebra we get

$$\frac{l+1}{l}\frac{j_{l+1}(Q)}{j_{l-1}(Q)}=1-\frac{\omega_p^2}{\omega_\alpha^2}=\frac{aQ^2}{1+aQ^2}\ , \tag{9}$$

where $Q=kR$ and $a=[\beta/(\omega_p R)]^2$. For an aluminum sphere of $R=7$ nm, $a\approx 10^{-4}$. Equation (9) is a simplified version of the result of Crowell and Ritchie[1] for a sphere embedded in a dielectric medium and it is also implicit in the work of Fujimoto and Komaki.[2] However, the results for surface and bulk modes when dispersion is included do not seem to have been worked out previously.

A. Surface modes

Surface modes ($\omega_\alpha<\omega_p$) correspond to imaginary values of Q ($=i\delta$). Except for a very small sphere the argument of the Bessel functions is large and they can be replaced by their asymptotic expression $j_l(i\delta)=i^l e^\delta/2\delta$ yielding the well-known result for ω_α,[1,7]

$$\omega_\alpha=\omega_p[l/(2l+1)]^{1/2}\ . \tag{10}$$

When the approximations leading to Eq. (10) remain valid, the surface mode frequencies are not affected by the β-dependent dispersion term. In Fig. 1 we show the surface $l=1,2,3$ modes as a function of the radius of an aluminum sphere ($\omega_p\simeq 0.56$). Our results show the same behavior as those of Boardman and Paranjape.[8] (See also Ref. 9.)

For $R\lesssim 100$ a.u., the R dependence of ω_α must be considered even if a local undispersed model is used for the response of the medium. For bulk modes, however, the R dependence of ω is only relevant for very small values of R ($R\lesssim 10$), but in this case a nonlocal potential must always be used.

B. Bulk modes

Bulk modes ($\omega_\alpha>\omega_p$) appear for real arguments of the Bessel function. From the well-known behavior of $j_l(\rho)$ we deduce that there is a solution lying in the range $\rho_{l+1,\nu}\le Q\le\rho'_{l,\nu+1}\le\rho_{l-1,\nu+1}$ where $\rho_{l,\nu}$ and $\rho'_{l,\nu}$ denote the νth root of $j_l(\rho)$ and $j'_l(\rho)$, respectively. The prime here indicates the derivative with respect to the argument. As Q increases from $\rho_{l+1,\nu}$ to $\rho'_{l,\nu+1}$ the left-hand side of Eq. (9) goes from 0 to 1. Since the difference between $\rho_{l+1,\nu}$ and $\rho_{l-1,\nu+1}$ is quite small for typical values of the parameters, we take $Q=\rho_{l+1,\nu}$ as a first approximation. This corresponds to zero field outside the sphere [see Eq. (8)] and is exact for $l=0$.

The bulk mode frequencies $\omega_\alpha=\omega_{l,\nu}$ are thus specified by a total angular component l and a radial component ν, each mode having a $2l+1$ degeneracy arising from the possible values of the azimuthal number m. For the l,ν mode the density fluctuation exhibits l angular and $\nu-1$ radial nodes.

The requirement of charge conservation for the sphere excludes the $\omega_{00}=\omega_p$ mode. This is also automatically fulfilled for $l\ge 1$ because the angular function averages to zero. For $l=0$, $\nu\neq 0$ we have

$$\int_0^R j_0(Qr/R)r^2dr=R^3 j_1(Q)/Q=0 \tag{11}$$

because $Q=\rho_{l+1,\nu}$.

Figure 2 shows for several modes the variation of $\omega_{l,\nu}$ with the sphere radius.

III. EXCITATION PROBABILITY

We can write the Hamiltonian of the free sphere

$$\mathrm{H}=\int \tfrac{1}{2}\left[n_0(\nabla\psi)^2-n\phi+\frac{\beta^2}{n_0}n^2\right]d^3r \tag{12}$$

in second quantization form in terms of the creation and annihilation operators of the modes. It allows us to determine the amplitude coefficient B_α for each mode:

$$B_\alpha=\left[\frac{4\pi\omega_p^2}{R^3\omega_\alpha|k|^2}\right]^{1/2}\left[(-1)^\gamma j_{l-1}(kR)j_{l+1}(kR)\left[\frac{2}{2l+1}\frac{\omega_p^2}{\omega_\alpha^2}+1\right]+(-1)^{\gamma+1}j_l^2(kR)\right]^{-1/2}\ , \tag{13}$$

where $\gamma=l$ for surface modes and $\gamma=-1$ for bulk modes.

In writing (12) we have assumed that the mean negative charge distribution cancels out point by point the positive jelli-

um over the whole volume of the sphere. The probability that the sphere be excited from the ground state $|0\rangle$ to an excited state $|\alpha\rangle$ after the passage of the fast electron is, in the Born approximation

$$W_\alpha = \left| \int_{-\infty}^{\infty} dt \langle \alpha | H_I | 0 \rangle \right|^2 , \tag{14}$$

where H_I is the interaction Hamiltonian

$$H_I = -\int \Psi_f^\dagger \phi(\mathbf{r},t) \Psi_i d^3 r \ . \tag{15}$$

Here Ψ_i and Ψ_f are field operators describing the initial and final electron states.

A. Classical probe

The incident particle is described as a point charge represented by a distribution density (see Fig. 3)

$$\langle \Psi_f^\dagger \Psi_i \rangle = \delta(x - x_0)\delta(y - y_0)\delta(z + vt) \ . \tag{16}$$

After a straightforward calculation, we obtain for the $l=1$, $m=0$ surface mode

$$W_{10}^C = \frac{2\omega_1^3 R^3}{v^4} K_0^2 \left[\frac{\omega_1}{v} b \right], \quad b \geq R \tag{17}$$

$$W_{10}^C = 2\omega_1 \left| \frac{R^{1/2}}{v} \sin(\omega_1 \tau) + \frac{v}{\omega_1^2} R^{-3/2} [\sin(\omega_1 \tau) - \omega_1 \tau \cos(\omega_1 \tau)] + \frac{\omega_1}{v^2} R^{3/2} \int_{v\tau}^{\infty} \frac{dx}{(x^2+b^2)^{1/2}} \cos\frac{\omega_1 x}{v} \right|^2 , \quad b \leq R \tag{18}$$

where K_0 is the modified Bessel function, $b=(x_0^2+y_0^2)^{1/2}$ is the electron impact parameter, and $\tau = 2(R^2-b^2)^{1/2}/v$ is the time the electron spends inside the sphere.

Equation (17) agrees with the first term of the expression obtained by Echenique and Ferrell[10] for the probability of energy loss by a classical electron with impact parameter b. They find that the probability of exciting a mode (l,m) when the incident electron is outside the sphere is proportional to $(\omega_l R/v)^{2l} K_m^2(\omega_l b/v)$. A detailed study of the number of modes excited using a realistic experimental dielectric response function has been made by Echenique *et al.*[11] To compare the classical results with those obtained considering a finite-size quantum probe, we integrate the point-particle result over a Gaussian distribution of classical trajectories,

$$P = \int |\Phi(\boldsymbol{\rho} - \mathbf{b})|^2 W^C(\boldsymbol{\rho}) d^2\rho \tag{19}$$

with $\boldsymbol{\rho}=(x,y)$, $\mathbf{b}=(x_0,y_0)$ and

$$|\Phi(\boldsymbol{\rho}-\mathbf{b})|^2 = \frac{2\nu}{\pi} \exp\{-2\nu[(x-x_0)^2+(y-y_0)^2]\} \tag{20}$$

and $\nu = 2.77/D^2$ (D being the Gaussian width).

In Fig. 4 are plotted the results of a numerical calculation of Eq. (19) as a function of the sphere radius for a fixed width $D=50$ a.u. and zero impact parameter.

Ritchie[12] has proved that the total probability for a quantum probe which is described by a Gaussian is equal

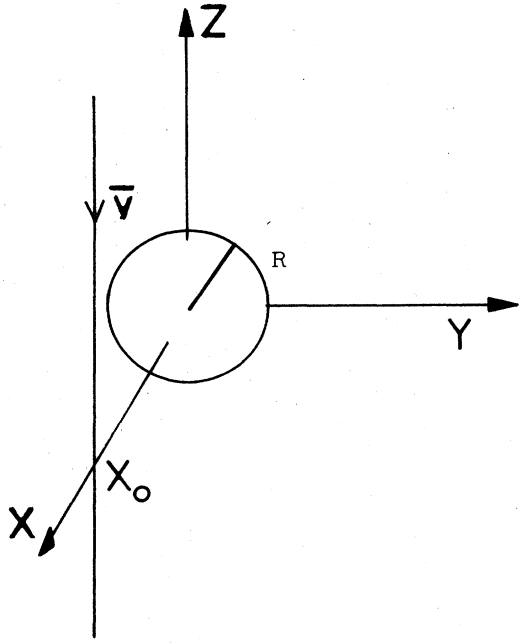

FIG. 3. Trajectory assumed for the incident electron.

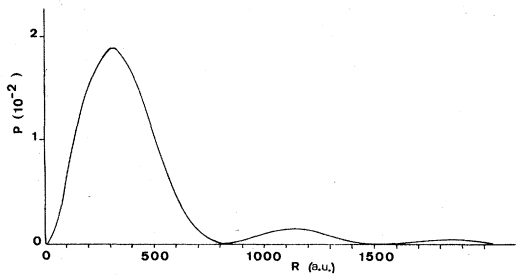

FIG. 4. Variation of the energy-loss probability P for the surface mode $l=1$, $m=0$ for a classical electron, against the sphere radius. The Gaussian distribution has a width $D=50$ a.u. Initial velocity $v=76.6$ a.u. and zero impact parameter.

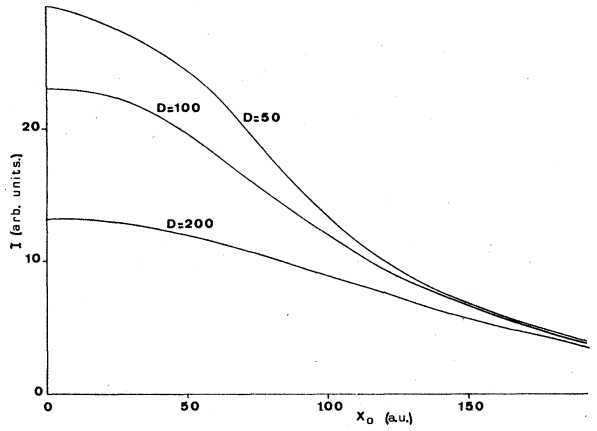

FIG. 5. Relative differential energy-loss probability along the incident direction for the $l=1$, $m=0$ mode against the impact parameter (see text). Several values of the width of the Gaussian distribution are considered. $v=76.6$ and $R=100$ a.u.

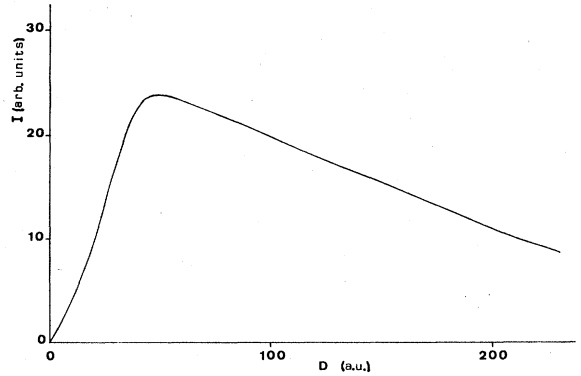

FIG. 6. Relative differential energy-loss probability along the incident direction for the $l=1$, $m=1$ mode as a function of the width of the Gaussian. $x_0=50$, $R=100$, and $v=76.6$ a.u.

to the integrated probability of classical trajectories with the same Gaussian distribution:

$$W_\alpha^Q(\mathbf{b})=\int |\Phi(\mathbf{b}-\boldsymbol{\rho})|^2 W_\alpha^C(\boldsymbol{\rho})d^2\rho \ . \tag{21}$$

To our knowledge there is no proof of an equivalent expression valid for a particular final direction. This is only valid after the Gaussian has been integrated over all final momentum values.

B. Quantum probe

The excitation probability is given by

$$W_\alpha^Q=\frac{2\pi L}{v}\sum_{k_f}|\langle f|\int d^3r\,\Psi_f^\dagger\langle\alpha|H_I|0\rangle\Psi_i|i\rangle|^2 \times\delta\left[\frac{k_i^2}{2}-\frac{k_f^2}{2}-\omega_\alpha\right] . \tag{22}$$

We take for Ψ_i and Ψ_f the following states:

$$\Psi_i(\mathbf{r},t)=\sum_{k_i}\left[\frac{2\nu}{\pi L}\right]^{1/2} e^{-\nu[(x-x_0)^2+y^2]}e^{-i\mathbf{k}_i\cdot\mathbf{r}}a_{\mathbf{k}_i}^\dagger \ ,$$
$$\Psi_f=\sum_{\mathbf{k}_f}(L)^{-3/2}e^{-i\mathbf{k}_f\cdot\mathbf{r}}a_{\mathbf{k}_f}^\dagger \ , \tag{23}$$

where L^3 is the normalization volume and $a_{\mathbf{k}}^\dagger$ is the electron creation operator.

The probability per unit solid angle is then given by

$$\frac{dW_\alpha^Q}{d\Omega}=\frac{\nu}{2\pi^3 v}(v^2-2\omega_\alpha)^{1/2} \times\left|\int d^3r\,e^{-iqz}\langle\alpha|H_I|0\rangle e^{-\nu[(x-x_0)^2+y^2]}\right|^2 , \tag{24}$$

where $q=v-(v^2-2\omega_\alpha)^{1/2}$ is the momentum transfer along the z direction.

To examine the influence of the probe size on the excitation probabilities for an aluminum sphere, we have evaluated $dW^Q/d\Omega$ numerically for several values of the relevant parameters and normalized them to the elastic scattering result [i.e., that obtained by changing the interaction Hamiltonian in Eq. (24) to the identity operator].

IV. RESULTS AND DISCUSSION

In Figs. 5–7 we show the dependence of the differential energy-loss probability

$$[I=(dW_\alpha^Q/d\Omega)_{\text{inelastic}}/(dW_\alpha^Q/d\Omega)_{\text{elastic}}]$$

of the $l=1$, $m=0,1$ modes upon the impact parameter and the width D of the Gaussian. The excitation probability is very much dependent on the mode excited and on the size of the probe as the experimental data of Batson and Treacy suggest.[13]

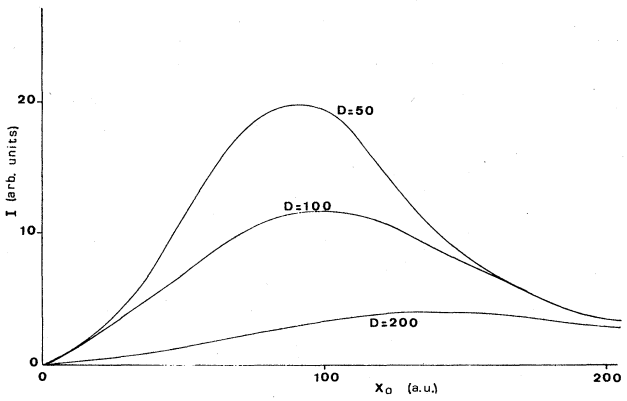

FIG. 7. The same as in Fig. 5 for the $l=1$, $m=1$ mode.

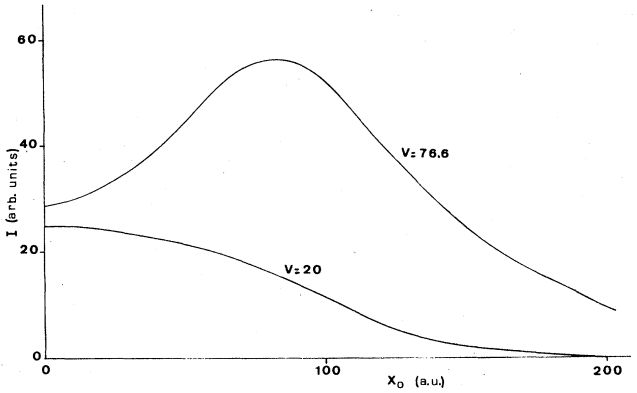

FIG. 8. The same as in Fig. 5 for the full $l=1$ mode. Several values of the velocity are considered. $D=50$ and $R=100$ a.u.

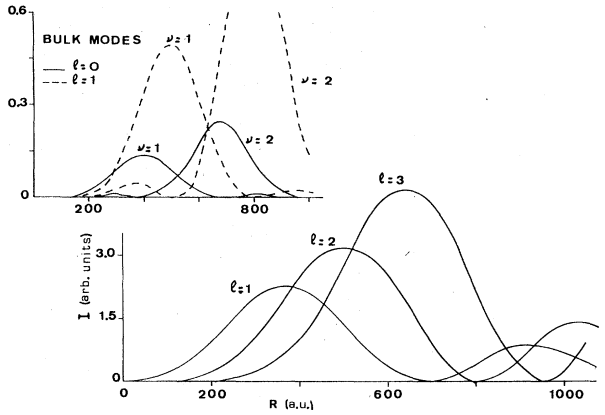

FIG. 10. Relative energy-loss probability for surface (big scale) and bulk (small scale) plasma excitations for several values of l and $\nu, m=0$. Incident plane wave.

For the $l=1$, $m=0$ case (Fig. 5) the highest excitation probability corresponds to small impact parameters ($x_0 \simeq 0$) as a logical consequence of the fact that the angular distribution $Y_{10}(\theta,\varphi)$ leads to significant values of the density fluctuation only along the z axis.

Figure 7 corresponds to the $l=1$, $m=1$ mode. For this mode the induced charge fluctuation lies in the equatorial plane of the sphere. It leads to a maximum excitation probability at values of the impact parameter close to the radius of the sphere, i.e., grazing incidence.

As the Gaussian width increases, the electron density decreases and therefore the excitation probability also decreases. However, this effect is balanced by the proportion of flux being scattered at grazing incidence,[14] as is shown in Fig. 6, where a beam centered at 50 a.u. strikes a sphere of radius $R=100$ a.u. The excitation probability initially increases with D, and reaches its maximum at $D=50$ a.u., corresponding to the beginning of grazing incidence and then decreases for greater values of D.

The total excitation probability of the dipole mode $l=1$ is shown in Fig. 8. The relative weight of each mode m depends on the ratio between v and $\omega_\alpha R$. For high velocities ($v=76.6$ a.u.) the largest contribution is due to the $m=1$ mode while for low velocities ($v=20$ a.u.) the $m=0$ dominates. This is in agreement with the results obtained by Kohl.[15]

Figure 9 shows the excitation probability as a function of the sphere radius for zero impact parameter and a width of 50 a.u. We obtain a structure of peaks of decreasing height as R increases. For each mode there are particular values of R for which there is a resonance effect.

According to our results the excitation of bulk modes is usually more important than that of the surface modes. This effect is a direct consequence of the incident beam geometry as is shown by using an incident plane wave instead of a Gaussian distribution (see Fig. 10). In Fig. 11 we plot for four values of the sphere radius the intensity of the different excited l modes.

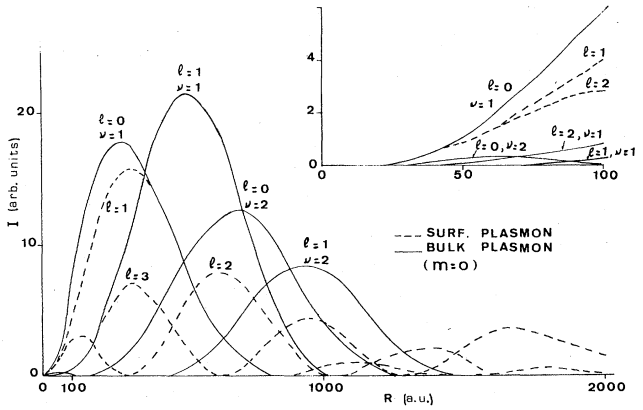

FIG. 9. Variation of the relative differential energy-loss probability with the radius R, for several surface and bulk modes. Zero impact parameter, $v=76.6$ and $D=50$ a.u.

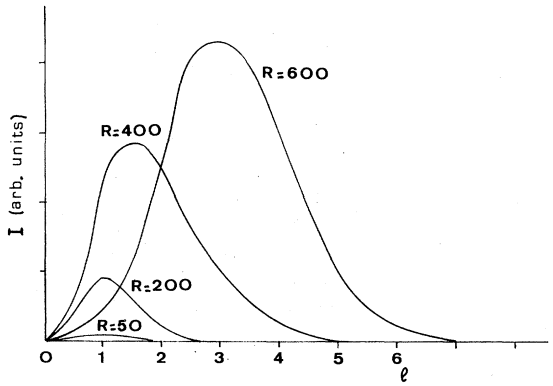

FIG. 11. Relative energy-loss probability for surface modes for a fixed radius R as a function of l (incident plane wave).

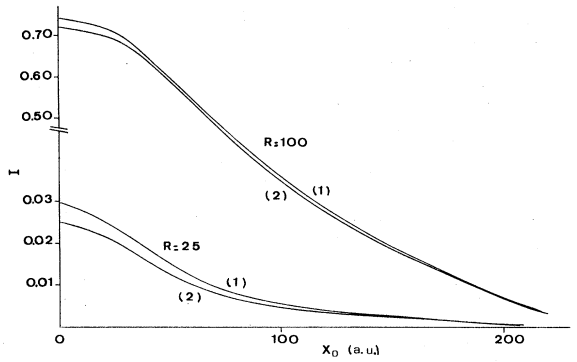

FIG. 12. Relative energy-loss probability of the $l=1$, $m=0$ surface mode for several values of R with (2) and without (1) dispersion effects. $D=50$ and $v=76.6$ a.u.

We want to make a final comment about the nonlocality. In this paper we have studied bulk and surface excitations separately. In the former case the β-dependent term, namely the plasmon dispersion, is always necessary to have interaction of the incident electron with the modes. In the latter case plasmon dispersion represents a small effect as is shown in Fig. 12 where the results of a calculation of the $l=1$, $m=0$ excitation probability are shown with and without dispersion terms. For most practical values of R, the excitation probability is roughly the same, dispersion effects being only relevant for very small spheres (about 13.5% for $R=13.2$ Å).

According to Penn and Apell[16] the full inclusion of electron-hole excitation is equivalent to allowing the surface density fluctuation to extend both into the solid and into the vacuum. The effect of extending the induced charge into the solid can be readily obtained by adding an extra term to Eq. (1) which becomes

$$\nabla\frac{\partial}{\partial t}\psi=-\nabla\phi+\frac{\beta^2}{n_0}\nabla n-\tfrac{1}{4}\nabla\left[\nabla^2\frac{n}{n_0}\right]. \tag{25}$$

The inclusion of this term allows us to recover the dispersion relation for the bulk modes of an infinite metal given by the plasmon pole approximation for the electron gas response,[17] i.e.,

$$\omega^2=\omega_p^2+\beta^2k^2+\tfrac{1}{4}k^4\,. \tag{26}$$

Finally, to allow the density fluctuation to extend into the vacuum region one should have a finite-step potential at the surface and $n(\mathbf{r})$ would have an exponential falloff for $r>R$. Since our main purpose has been to study the correlation between probe geometry, nature of the modes and the energy-loss spectra, this is beyond our scope. It has been claimed[16] that nonlocality might change the absolute value of the excitation probability by an order of magnitude. Nevertheless, we expect this effect will not change our results qualitatively. Further work along these lines is in progress.

ACKNOWLEDGMENTS

We want to express our gratitude to Dr. Archie Howie for his guidance and helpful discussions in most parts of this work. Helpful conversations in connection with this work with R. H. Ritchie are gratefully acknowledged. One of us (N.B.) would like to acknowledge the Comisión Asesora de Investigación y Ciencia (Spain) as well as the British Council in Barcelona for financial support.

[1]J. Crowell and R. H. Ritchie, Phys. Rev. **172**, 436 (1968).
[2]F. Fujimoto and K. Komaki, J. Phys. Soc. Jpn. **25**, 1679 (1968).
[3]P. E. Batson, Solid State Commun. **34**, 477 (1980).
[4]M. Schmeits, J. Phys. C **14**, 1203 (1981).
[5]R. H. Ritchie and R. E. Wilems, Phys. Rev. **178**, 372 (1969).
[6]F. Forstmann, Z. Phys. **32**, 385 (1979).
[7]G. Mie, Ann. Phys. (Leipzig) **25 (4)**, 377 (1908).
[8]A. D. Boardman and B. V. Paranjape, J. Phys. F **7**, 1935 (1977).
[9]W. Jaisli, H. Kuhlman, and G. Schultz-Ekloff, Surf. Sci. **112**, L797 (1981).
[10]P. M. Echenique and T. Ferrell (unpublished).
[11]P. M. Echenique, A. Howie, R. Milme, and D. Wheatley (unpublished).
[12]R. H. Ritchie (unpublished).
[13]P. E. Batson and M. M. J. Treacy, in *Proceedings of the Electron Microscopy Society of America, San Francisco, 1980* (Claitor's, Baton Rouge, 1980), p. 126.
[14]The importance of grazing incidence was pointed out by P. E. Batson, in *Proceedings of the Electron Microscopy Society of America, San Francisco, 1980,* Ref. 13.
[15]H. Kohl, Ultramicroscopy **II**, 53 (1983).
[16]Q. R. Penn and P. Apell, J. Phys. C **16**, 5729 (1983).
[17]B. I. Lundqvist, Phys. Kondens. Mater. **6**, 206 (1967).